Provided for non-commercial research and education use.
Not for reproduction, distribution or commercial use.

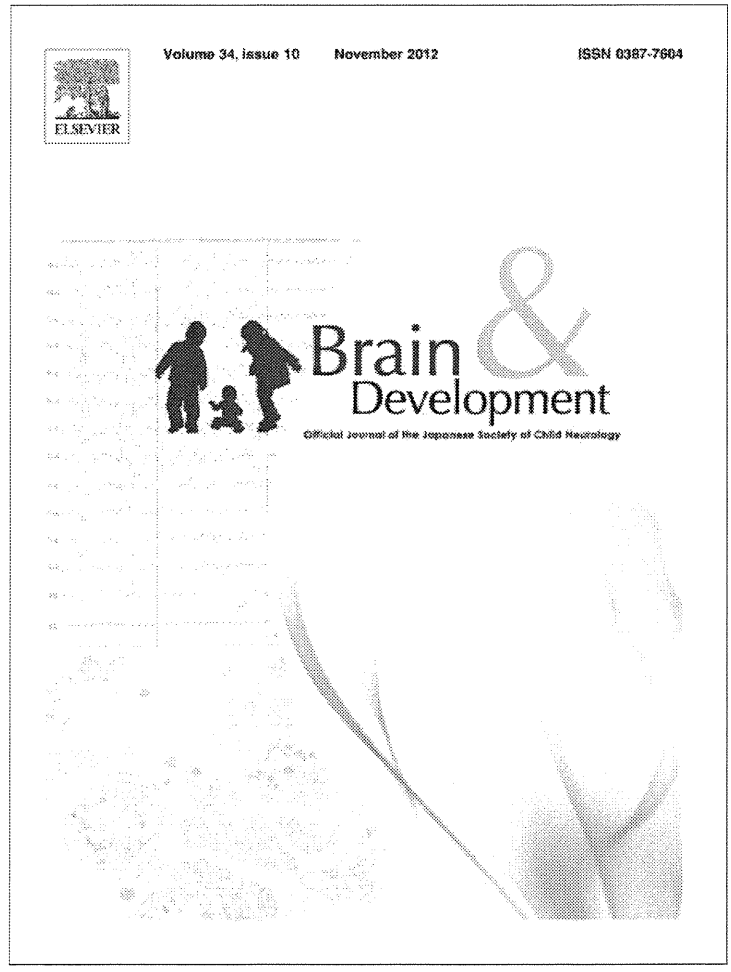

This article appeared in a journal published by Elsevier. The attached copy is furnished to the author for internal non-commercial research and education use, including for instruction at the authors institution and sharing with colleagues.

Other uses, including reproduction and distribution, or selling or licensing copies, or posting to personal, institutional or third party websites are prohibited.

In most cases authors are permitted to post their version of the article (e.g. in Word or Tex form) to their personal website or institutional repository. Authors requiring further information regarding Elsevier's archiving and manuscript policies are encouraged to visit:

http://www.elsevier.com/copyright

Author's personal copy

ELSEVIER

Brain & Development 34 (2012) 881–885

BRAIN & DEVELOPMENT
Official Journal of the Japanese Society of Child Neurology

www.elsevier.com/locate/braindev

Case report

A severe form of epidermal nevus syndrome associated with brainstem and cerebellar malformations and neonatal medulloblastoma

Akihisa Okumura [a,*], Tsubasa Lee [a], Mitsuru Ikeno [a], Keiko Shimojima [b], Kazunori Kajino [c], Yuka Inoue [a], Naomi Yoshikawa [a], Hiroki Suganuma [a], Mitsuyoshi Suzuki [a], Ken Hisata [a], Hiromichi Shoji [a], Jun-ichi Takanashi [d], A. James Barkovich [e], Toshiaki Shimizu [a], Toshiyuki Yamamoto [b], Masaharu Hayashi [f]

[a] *Department of Pediatrics, Juntendo University Faculty of Medicine, Japan*
[b] *Tokyo Women's Medical University Institute for Integrated Medical Sciences, Japan*
[c] *Department of Pathology, Juntendo University Faculty of Medicine, Japan*
[d] *Department of Pediatrics, Kameda Medical Center, Japan*
[e] *Neuroradiology Section, Department of Radiology and Biomedical Imaging, University of California, San Francisco, CA, USA*
[f] *Department of Brain Development and Neural Regeneration, Tokyo Metropolitan Institute of Medical Science, Japan*

Received 9 January 2012; received in revised form 23 February 2012; accepted 6 March 2012

Abstract

Here we report a boy with epidermal nevus syndrome associated with brainstem and cerebellar malformations and neonatal medulloblastoma. The patient had epidermal nevi and complicated brain malformations including macrocephaly with polymicrogyria, dysmorphic and enlarged midbrain tectum, enlarged cerebellar hemispheres with small and maloriented folia. The patient died after surgical resection of medulloblastoma which was newly recognized on MRI at 51 days of age. Postmortem pathological examinations showed very unique and bizarre malformation of the midbrain and hindbrain. The cerebellar cortex exhibited a coarse, irregular and bumpy surface, blurred border between the Purkinje cell layer and internal granule cell layer, and many foci of heterotopia in the cerebellar white matter. The brainstem showed multiple anomalies, including enlargement of superior colliculi, hypoplasia of pyramidal tracts and dysplasia of inferior olivary nuclei. The unusual constellation of brain malformations of our patient will widen the spectrum of epidermal nevus syndrome.
© 2012 The Japanese Society of Child Neurology. Published by Elsevier B.V. All rights reserved.

Keywords: Epidermal nevus; Medulloblastoma; Cerebellar anomaly; Brainstem anomaly

1. Introduction

Epidermal nevus syndrome (ENS) is a rare neurocutaneous syndrome consisting of epidermal nevi and a variety of congenital defects in the brain, connective tissue, and ocular, skeletal, cardiac, genitourinary, and even endocrine systems [1–3]. A wide spectrum of brain abnormalities has been reported in ENS including unilateral hemimegalencephaly, vascular malformations, agenesis of the corpus callosum, and Dandy–Walker malformation [1,4,5]. We recently encountered an infant with the unusual constellation of epidermal nevi, severe neuronal migration abnormalities in the cerebrum and

* Corresponding author. Address: Department of Pediatrics, Juntendo University Faculty of Medicine, 2-1-1 Hongo, Bunkyo-ku, Tokyo 113-8421, Japan. Tel.: +81 3 3813 3111; fax: +81 3 5800 1580.
E-mail address: okumura@juntendo.ac.jp (A. Okumura).

0387-7604/$ - see front matter © 2012 The Japanese Society of Child Neurology. Published by Elsevier B.V. All rights reserved.
http://dx.doi.org/10.1016/j.braindev.2012.03.003

Author's personal copy

cerebellum, and neonatal medulloblastoma. Here we report neuroimaging and pathological findings of this infant.

2. Patient report

2.1. Clinical course

The patient was a boy born after 38 weeks of gestation with birthweight of 3540 g. He is the first child of non-consanguineous healthy parents. Macrocephaly and enlarged fourth ventricle were noted on fetal ultrasonography at 22 weeks of gestation. He was delivered by scheduled caesarean section because of macrocephaly. His Apgar score was 9 at 5 min. He was admitted to our hospital because of unstable respiration and macrocephaly.

On admission, marked macrocephaly with head circumference of 40.0 cm (+4.6 SD), tachypnea with retraction, and general hypotonia were recognized. Flesh-colored verrucous plaques were present on his neck, left scapular area, and lower back (Fig. 1A). Routine blood cell counts and chemistry were unremarkable. Serum lactate, pyruvate, and ammonia levels were within normal range. Metabolic screening for amino and organic acid analyses was also unremarkable. Array-comparative genomic hybridization analysis using Human Genome CGH Microarray 105A chip revealed no genomic copy number aberrations.

Head CT on the first day of life (Fig. 2A and B) revealed poor gyral formation with few and shallow sulci. The lateral ventricles were mildly dilated and the fourth ventricle dysmorphic and enlarged. Abnormally increased attenuation, presumed to be calcification, was identified in the left frontal lobe and both cerebellar hemispheres. MRI on the same day revealed a dysmorphic, enlarged midbrain tectum with disproportionately enlarged inferior colliculi (Fig. 2C); a small cerebellum that wrapped around the brain stem ventrally and had small and maloriented folia (Fig. 2D); and polymicrogyria affecting much of the right cerebral hemisphere (Fig. 2E and F). The subcortical white matter of the left frontal lobe was abnormally hyperintense on T1-weighted images and hypointense on T2-weighted images, suggesting calcification. The corpus callosum was markedly T1 hyperintense and thick in its anterior half. The caudate and lentiform nuclei were poorly differentiated from the surrounding structures.

EEG 3 h after birth showed ictal changes with continuous rhythmic theta waves in the left frontal area. Although no convulsive movement was observed, his respiration was irregular and a fluctuation of blood pressure was recognized. Ictal EEG changes were subsided with intravenous phenobarbital and his vital signs were stabilized simultaneously. Thus, autonomic instability was considered to be caused by seizures. Background EEG activities were markedly abnormal without physiological wave forms. Subclinical seizures from the left frontal areas were occasionally observed on serial EEGs.

His general condition gradually improved, although he required mechanical ventilation for 16 days and

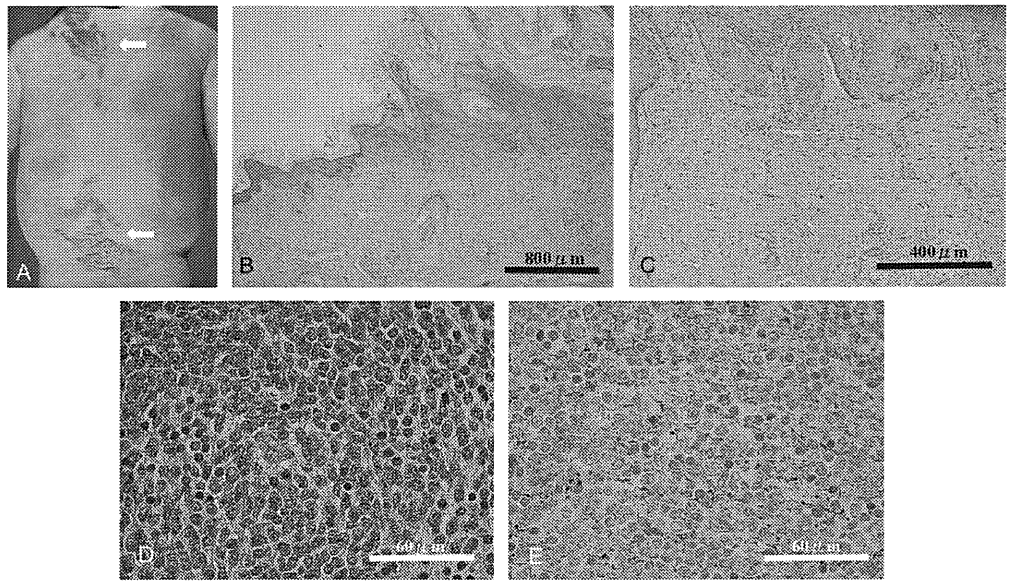

Fig. 1. Skin and tumor. (A) The back of the patient. Verrucous plaques (arrows) were present on his neck, left scapular area, and lower back. (B and C) The skin showed papillomatous epidermal hyperplasia, hyperkeratosis and hypergranulosis (B, bar = 800 μm), in addition to abnormal folliculosebaceous glands (C, bar = 400 μm), hematoxylin eosin staining. (D and E) Histology of the tumor. Densely packed cells with highly chromatic nuclei and scanty cytoplasm were seen (D, bar = 60 μm, hematoxylin eosin staining). Coarse granules was visualized by immunohistochemistry for synaptophysin (E, bar = 60 μm).

Author's personal copy

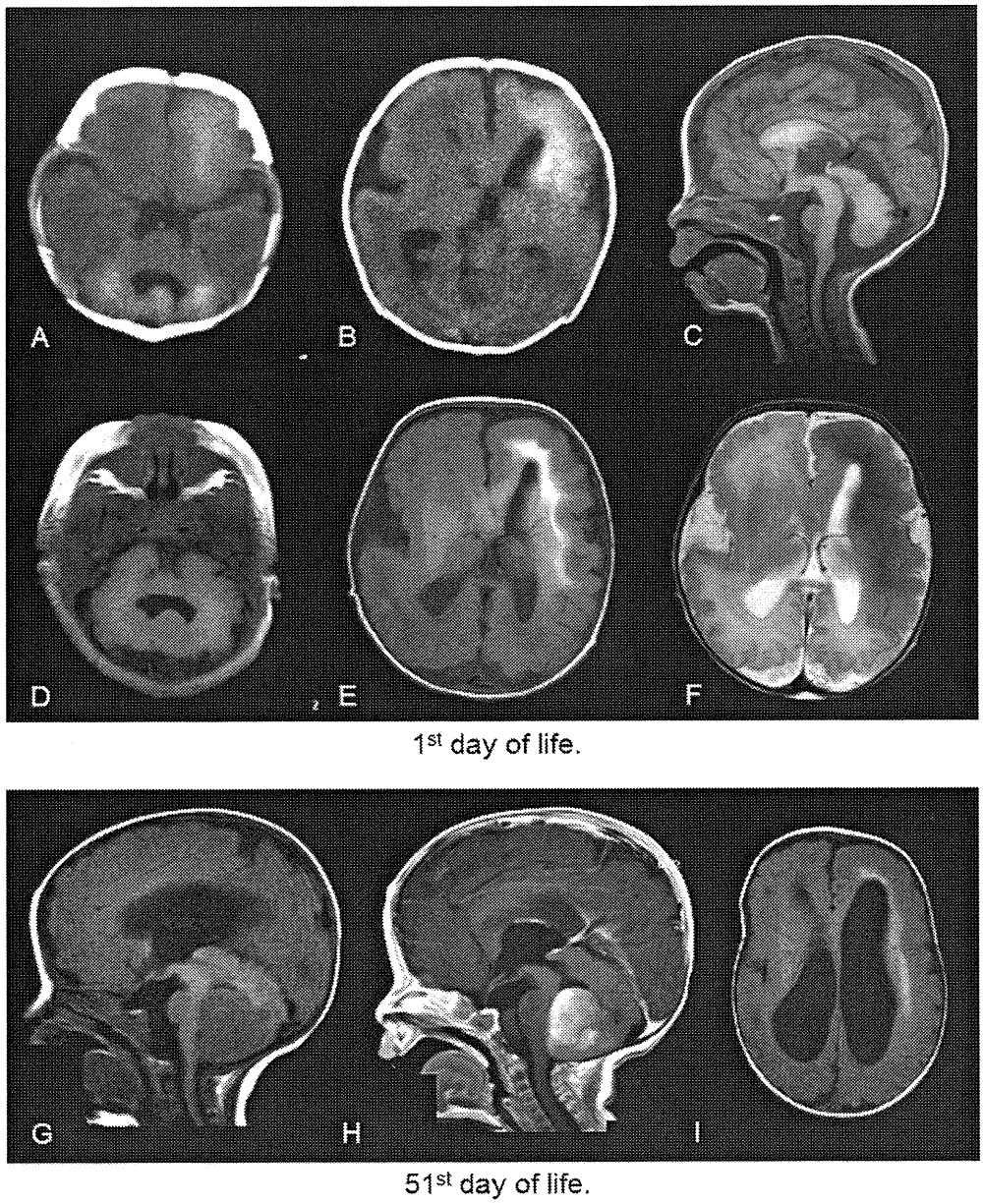

Fig. 2. Neuroimaging findings. (A and B) CT on the first day of life. Poor gyral formation, aberrant fourth ventricle, and high densities in the left frontal area and cerebellar hemispheres were observed. (C–F) MRI on the first day of life. The corpus callosum was markedly hypertrophic in the anterior half (C). The mesencephalic tectum was enlarged and dysmorphic, and the pons was small (C). The cerebellar vermis was small and dysmorphic with insufficient folia formation (C).The cerebellar hemispheres were enlarged and wrapped around the brainstem (D). The cortical surface was smooth and gyral formation was poor (E and F). Caudate and lentiform nuclei were poorly differentiated from the surrounding structures (E and F). (G–I) MRI on the 51th day of life. A mass lesion was present at the posterior wall of the fourth ventricle (G). Tumor was enhanced by paramagnetic contrast agent (H). Ventriclomegaly with ballooning of ventricular walls was observed (I).

nasogastric feeding for 30 days. However, his head circumference had been rapidly increasing since 35 days of age. MRI on 51 days of age demonstrated marked lateral and third ventricular hydrocephalus caused by an enhancing mass lesion in the fourth ventricle (Fig. 2G–I). Surgical resection was performed on 56 days of age. Tumor histology was diagnostic of medulloblastoma. He died of a worsening of general conditions after surgery on 57 days of age.

2.2. Pathological examination

Examination of the skin showed epidermal hyperplasia (Fig. 1A), hyperkeratosis, hypergranulosis, and abnormal folliculo-sebaceous glands (Fig. 1B and C), leading to the diagnosis of epidermal nevus (nevus sebaceous).

The surgical specimen of tumor consisted of densely packed carrot shaped cells with highly chromatic nuclei

Author's personal copy

surrounded by scanty cytoplasm (Fig. 1D). The tumor had rare rosette formation and included a few reticulin positive fibers. Neuronal differentiation was identified by immunohistochemistry for synaptophysin (Fig. 1E). The diagnosis was classic medulloblastoma.

The brain weighed 970 g after formalin fixation. The left frontal pole, the right temporal pole and insular cortex, and the bilateral paracentral cortex were agyric, while the orbital surface of the frontal lobe and parietal cortex demonstrated polymicrogyria (Fig. 3A). The olfactory bulbs and tracts were widened. The corpus callosum was hypoplastic (Fig. 3B). The ventral cerebellum was multilobulated and displaced ventrally to the upper brainstem (Fig. 3C). The vermis was not identified due to surgical resection. The caudal surface of cerebellum had irregular nodular bumps.

Histologically, the agyric cerebral cortex consisted of cell-sparse molecular layer, superficial neuronal layer and deep columnar distribution of neurons. The polymicrogyric cortex showed fused molecular layer across gyri (Fig. 3D). The bilateral caudate nuclei were enlarged, showed irregular myelinated fibers, and much perivascular pseudocalcification (Fig. 3E). The subnuclei were not differentiated in the thalamus.

The cerebellar cortex showed a blurred junction of the Purkinje cell and internal granular layers, and ectopic Purkinje cells within the internal granule layer (Fig. 3F and G). Foci of heterotopia, consisting of apparent Purkinje cells and granule cells, were scattered in the white matter, and the dentate nuclei were not identified. The superior colliculus was large, and the middle cerebellar peduncles were ventrally displaced (Fig. 3H). The cerebral crus, pontine longitudinal fasciculus and medullary pyramids were hypoplastic. The inferior olivary nucleus showed plump undulation (Fig. 3I).

3. Discussion

Central nervous system involvement in ENS varies widely among the patients. Abdelhalim et al. reported an infant with ENS characterized by enlargement of both cerebral hemispheres, malformed basal ganglia, and unilateral enlargement of cerebellar hemisphere

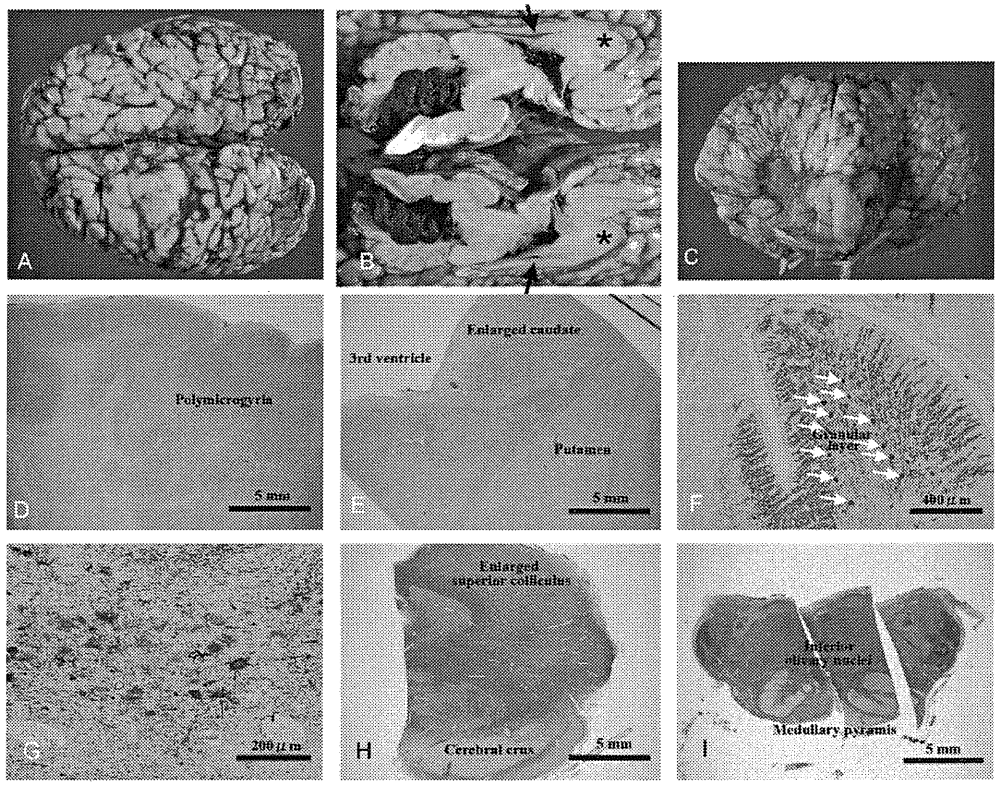

Fig. 3. Neuropathological findings. (A) The bilateral paracentral cortex was agyric. (B) Midline section. The anterior part of the corpus callosum (asterisks) was thickened, whereas the posterior portion (arrows) was thinned. (C) The rostral part of cerebellum was lumpish and displaced ventrally to the upper brainstem. (D) The orbital cortex demonstrated polymicrogyria, Klüver–Barrea staining, bar = 5 mm. (E) The left caudate nucleus was enlarged in comparison with the putamen, hematoxylin eosin staining, bar = 5 mm. (F) The cerebellar cortex showed blurred differentiation between the ectopic Purkinje cell (arrows) and the internal granular layer, calbindin-D28K immunostaining, bar = 400 μm. (G) Heterotopia in the cerebellum consisted of apparent Purkinje cells, which were immunoreactive for calbindin-D28K, bar = 200 μm. (H) The upper midbrain showed enlargement of the superior colliculus and hypoplasia of the cerebral crus, respectively, Klüver–Barrea staining, bar = 5 mm. (I) The upper medulla oblongata demonstrated dysplastic undulation of the inferior olivary nuclei, in addition to hypoplasia in the pyramis, Klüver–Barrea staining, bar = 5 mm.

Author's personal copy

with disorganized folia [6]. The neuroimaging and macroscopic pathological findings have some similarities to those of our patient, but their patient lacked severe brainstem anomalies and medulloblastoma. These two cases may represent a very severe form of ENS.

Our patient demonstrated very unique and bizarre malformation of the midbrain and hindbrain, which is very different from previous cases reported in conjunction with ENS. The cerebellar cortex was grossly abnormal, exhibiting a coarse, irregular and bumpy surface. Histologically, the border between the Purkinje cell layer and internal granule cell layer was blurred in the cerebellar cortex, and there were many foci of heterotopia in the cerebellar white matter. The brainstem also showed multiple anomalies, including enlargement of superior colliculi, hypoplasia of pyramidal tracts and dysplasia of inferior olivary nuclei. Pereira et al. reported the association of enlargement and disorganized folia in the left cerebellum in a 24-year-old patient with ENS [7]. Since the occurrence of infratentorial anomalies has only rarely been reported in ENS [6,7], the combination of supratentorial dysgenesis, infratentorial dysgenesis, and neonatal medulloblastoma in this patient is intriguing.

The Purkinje cells and some neurons of the deep cerebellar nuclei are GABAergic neurons that arise from the ventricular zone of metencephalic alar plate between 6 and 18 gestational weeks, while granule cells and other glutamatergic neurons arise in the anterior rhombic lips starting at around 19 gestational weeks. Some neurons from the rhombic lip migrate into the transient external granular layer of the cerebellum, while others migrate into a nuclear transitory zone from which they will eventually migrate to the deep cerebellar nuclei. The external granular layer persists until after birth and functions as a secondary germinal zone in which the granule cells undergo multiple mitoses before they eventually migrate inward through the molecular and Purkinje cell layers to form the definitive granule cell layer of the mature cerebellar cortex [8]. In our patient, the formation of Purkinje cells and granule cells per se seemed to be spared, regardless of the ectopic distribution. The aberrant cerebellar formation in our patient was presumed to have occurred around 18–19 gestational weeks, although its pathogenesis is difficult to determine at present.

Another striking feature of our patient is development of neonatal medulloblastoma. Medulloblastomas extremely rarely present in neonates [9,10]. Recent studies have revealed somatic mosaicism for mutation of several oncogenes in patients with ENS and its related syndromes [11,12]. Bourdeaut et al. reported an oncogenic *KRAS* mutation in a patient with ENS associated with rhabdomyosarcoma [13]. These facts suggest that mutation(s) of some oncogene is likely to have participated in the pathogenesis of the syndrome manifested by our patient.

Acknowledgement

We thank Professor William Dobyns (Department of Human Genetics, University of Chicago, Chicago) and Professor Ilona J. Frieden (Department of Dermatology, University of California, San Francisco) for the useful suggestion for the diagnosis of the patient.

This study is supported by the Grant-in-aid for Research on Measures for Intractable Diseases, No. H23-Nanji-Ippan-073, from the Ministry of Health, Labour and Welfare, Japan.

References

[1] Pavone L, Curatolo P, Rizzo R, Micali G, Incorpora G, Garg BP, et al. Epidermal nevus syndrome: a neurologic variant with hemimegalencephaly, gyral malformation, mental retardation, seizures, and facial hemihypertrophy. Neurology 1991;41:266–71.
[2] Grebe TA, Rimsza ME, Richter SF, Hansen RC, Hoyme H. Further delineation of the epidermal nevus syndrome: two cases with new findings and literature review. Am J Med Genet 1993;47:24–30.
[3] Herman TE, Siegel MJ. Hemimegalencephaly and linear nevus sebaceous syndrome. J Perinatol 2001;21:336–8.
[4] Hennekam RC, Kwa VI, van Amerongen A. Arteriovenous and lymphatic malformations, linear verrucous epidermal nevus and mild overgrowth: another hamartoneoplastic syndrome? Clin Dysmorphol 1999;8:111–5.
[5] Dodge NN, Dobyns WB. Agenesis of the corpus callosum and Dandy-Walker malformation associated with hemimegalencephaly in the sebaceous nevus syndrome. Am J Med Genet 1995;56:147–50.
[6] Abdelhalim AN, Moritani T, Richfield E, Ekholm SE, Westesson PL. Epidermal nevus syndrome: megalencephaly with bihemispheric and cerebellar involvement: imaging and neuropathologic correlation. J Comput Assist Tomogr 2003;27:534–7.
[7] Pereira S, Serra D, Freitas PM, Santiago D, Brito O. Epidermal nevus syndrome: an unusual cerebellar involvement. J Neuroradiol 2009;36:237–9.
[8] Fink AJ, Englund C, Daza RA, Pham D, Lau C, Nivison M, et al. Development of the deep cerebellar nuclei: transcription factors and cell migration from the rhombic lip. J Neurosci 2006;26:3066–76.
[9] Ermis B, Aydemir C, Taspinar O, Cagavi F, Bahadir B, Ozdemir H. Congenital medulloblastoma. Arch Dis Child Fetal Neonatal Ed 2006;91:F373.
[10] Kayama T, Yoshimoto T, Shimizu H, Sakurai Y. Neonatal medulloblastoma. J Neurooncol 1993;15:157–63.
[11] Hafner C, López-Knowles E, Luis NM, Toll A, Baselga E, Fernández-Casado A, et al. Oncogenic PIK3CA mutations occur in epidermal nevi and seborrheic keratoses with a characteristic mutation pattern. Proc Natl Acad Sci USA 2007;104:13450–4.
[12] Hafner C, van Oers JM, Vogt T, Landthaler M, Stoehr R, Blaszyk H, et al. Mosaicism of activating FGFR3 mutations in human skin causes epidermal nevi. J Clin Invest 2006;116:2201–7.
[13] Bourdeaut F, Hérault A, Gentien D, Pierron G, Ballet S, Reynaud S, et al. Mosaicism for oncogenic G12D KRAS mutation associated with epidermal nevus, polycystic kidneys and rhabdomyosarcoma. J Med Genet 2010;47:859–62.

Provided for non-commercial research and education use.
Not for reproduction, distribution or commercial use.

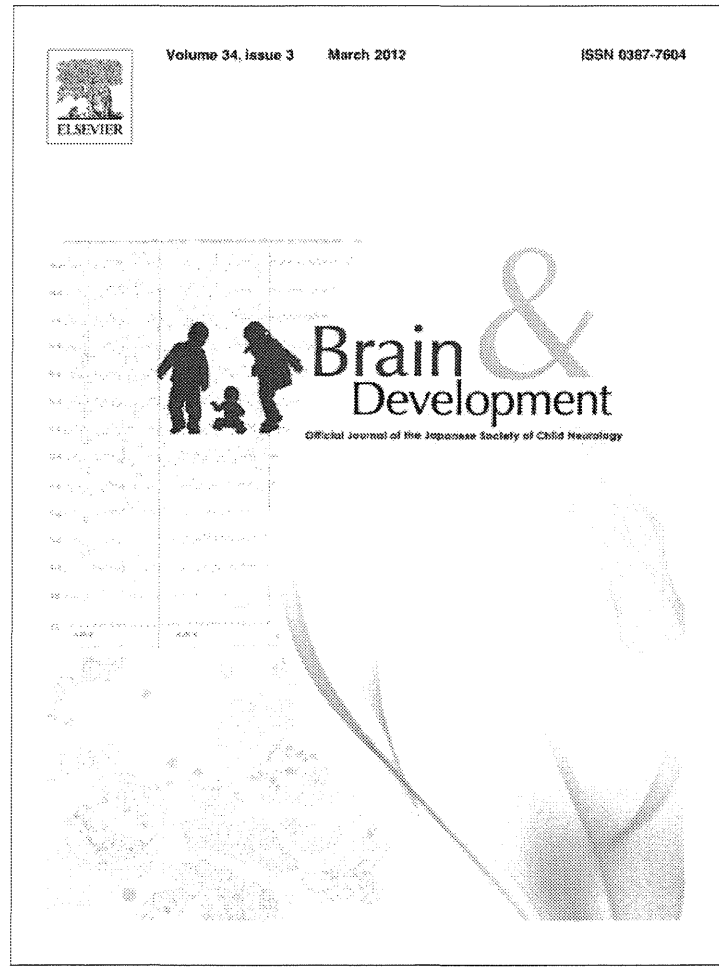

This article appeared in a journal published by Elsevier. The attached copy is furnished to the author for internal non-commercial research and education use, including for instruction at the authors institution and sharing with colleagues.

Other uses, including reproduction and distribution, or selling or licensing copies, or posting to personal, institutional or third party websites are prohibited.

In most cases authors are permitted to post their version of the article (e.g. in Word or Tex form) to their personal website or institutional repository. Authors requiring further information regarding Elsevier's archiving and manuscript policies are encouraged to visit:

http://www.elsevier.com/copyright

Author's personal copy

ELSEVIER

Brain & Development 34 (2012) 230–233

BRAIN & DEVELOPMENT
Official Journal of the Japanese Society of Child Neurology

www.elsevier.com/locate/braindev

Case report

Spinocerebellar ataxias type 27 derived from a disruption of the fibroblast growth factor 14 gene with mimicking phenotype of paroxysmal non-kinesigenic dyskinesia

Keiko Shimojima [a], Akihisa Okumura [b], Jun Natsume [c], Kaori Aiba [d], Hirokazu Kurahashi [e], Tetsuo Kubota [f], Kenji Yokochi [g], Toshiyuki Yamamoto [a,*]

[a] *Tokyo Women's Medical University Institute for Integrated Medical Sciences, Tokyo, Japan*
[b] *Department of Pediatrics, Juntendo University School of Medicine, Tokyo, Japan*
[c] *Department of Pediatrics, Nagoya University Graduate School of Medicine, Nagoya, Japan*
[d] *Department of Pediatrics, Toyohashi Municipal Hospital, Toyohashi, Japan*
[e] *Department of Pediatric Neurology, Aichi Prefectural Colony Central Hospital, Kasugai, Japan*
[f] *Department of Pediatrics, Anjo Kosei Hospital, Anjo, Japan*
[g] *Department of Pediatrics, Seirei-Mikatahara General Hospital, Hamamatsu, Shizuoka, Japan*

Received 17 November 2010; received in revised form 27 April 2011; accepted 27 April 2011

Abstract

Many types of spinocerebellar ataxias (SCAs) manifest as progressive disorders with cerebellar involvement. SCA type 27 (SCA27) is a rare type of SCA caused by mutations in the fibroblast growth factor 14 gene (*FGF14*). *FGF14* disruption caused by a de novo reciprocal chromosomal translocation between chromosomes 13 and 21 was identified in a patient with the phenotype of paroxysmal non-kinesigenic dyskinesia (PNKD). This indicated genetic heterogeneity of PNKD, since 60% of the patients with PNKD exhibit mutations in another gene responsible for PNKD, the myofibrillogenesis regulator 1 gene (*MR-1*). We hypothesized that the remaining 40% of patients with PNKD may have *FGF14* mutations; therefore, the nucleotide sequences of *MR-1* and *FGF14* were analyzed in another six patients with PNKD, but no nucleotide alterations were observed in these genes for these patients. Further studies should be conducted on the phenotypic heterogeneity of *FGF14* mutations and/or haploinsufficiency in SCA27 and PNKD.
© 2011 The Japanese Society of Child Neurology. Published by Elsevier B.V. All rights reserved.

1. Introduction

Spinocerebellar ataxias (SCAs) are progressive disorders that manifest as cerebellar symptoms such as gait ataxia, stance ataxia, dysmetria and/or kinetic tremor in all four limbs, as well as oculomotor deficits (nystagmus and hypermetria/hypometria of saccades) [1]. SCAs exhibit genetic heterogeneity, and at least 29 types of SCAs have been recognized to date [2]. Most of the subtypes show autosomal dominant traits, while some show anticipation due to triplet repeats. Therefore, onset age depends not only on the genetic subtypes but also on the mutation types. Since SCAs cannot be diagnosed solely on the basis of clinical evaluation, knowledge of the family history is very important for diagnosis of SCAs. However, if the patient is a small child with negative family history, it is extremely difficult to arrive at a final diagnosis.

* Corresponding author. Address: Tokyo Women's Medical University Institute for Integrated Medical Sciences, 8-1 Kawada-cho, Shinjuku-ward, Tokyo 162-8666, Japan. Tel.: +81 3 3353 8111x24013; fax: +81 3 5269 7667.
E-mail address: toshiyuki.yamamoto@twmu.ac.jp (T. Yamamoto).

0387-7604/$ - see front matter © 2011 The Japanese Society of Child Neurology. Published by Elsevier B.V. All rights reserved.
doi:10.1016/j.braindev.2011.04.014

Author's personal copy

Table 1
Summary of FISH analyses.

Band	BAC probe	Start	End	Result	
13q14.11	RP11-13I8	41,402,236	41,593,291	Marker	
13q33.1	RP11-180C7	101,579,849	101,742,909	Normal	
	RP11-230O10	101,668,810	101,837,797	***Disruption***	Covering *FGF14*
	RP11-1005B17	101,752,504	101,933,396	Translocation	
	RP11-46I10	101,854,462	102,028,883	Translocation	
	RP11-29B2	102,007,252	102,165,732	Translocation	
	RP11-2L10	102,337,773	102,514,754	Translocation	
13q34	RP11-569D9	113,930,807	114,103,243	Translocation	
21q22.12	RP11-272A3	34,768,332	34,953,503	Marker	
21q22.13	RP11-105O24	37,717,328	37,872,927	Marker	
21q22.3	RP11-34P17	46,391,180	46,582,695	***Disruption***	
	RP11-71A7	46,607,929	46,756,333	Translocation	
	RP11-433E24	46,717,198	46,912,065	Translocation	

Genome location corresponds to the March 2006 human reference sequence (NCBI Build 36).

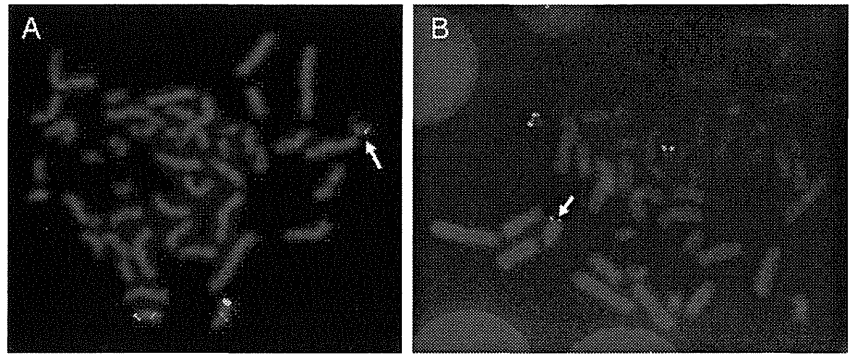

Fig. 1. Cytogenetic investigations for the breakpoints. (A) The one of the split signals of RP11-230O10 covering *FGF14* were identified on chromosome 21 (arrow). (B) The additional signals of RP11-34P17 located on 21q22.3 were identified on chromosome 13 (arrow).

We recently encountered a child who had paroxysmal non-kinesigenic dyskinesia (PNKD, MIM #118800) and exhibited a de novo reciprocal chromosomal translocation that caused a disruption in the fibroblast growth factor 14 gene (*FGF14*) responsible for SCA type 27 (SCA27, MIM #609307). In this study, we analyzed the responsible genes for PNKD including *FGF14* in other patients after obtaining permission from the ethical committee of our institution.

2. Case report

We encountered a boy (age, 3 years 9 months) who was referred to our institution for medical examination. He was born at 40 weeks of gestation, with a birth weight of 3370 g (75th–90th centile), height of 51 cm (75th–90th centile), and a head circumference of 32.5 cm (10th–25th centile). He underwent uneventful development until he was 8 months old. At this age, he started experiencing episodic attacks of muscle atonus and upward turning of both eyes; these episodes were triggered by intense crying and occurred several times a week. These episodes were diagnosed as breath-holding spells, and the patient underwent therapy with valproic acid and phenobarbital on increase in the frequency of these episodes. When the patient was admitted to the hospital, his stature was within normal limits for his age; his weight was 15.6 kg (50th–75th centile), height was 99.5 cm (50th–75th centile), and head circumference was 49.2 cm (25th–50th centile). Intermediate time of episodes, he did not exhibit any neurological symptoms except for hyperkinetic behaviors. Immediately after crying, the patient exhibited involuntary gross movements of the extremities, associated with choreic movements of the head and truncus. During these episodes, which usually lasted for approximately 5 min, he was alert and could reply when his name was called out. Laboratory tests, including routine blood and urine tests; radiological tests, including brain magnetic resonance imaging and magnetic resonance angiography; and electroencephalography yielded normal results. At the age of 6 years, the patient's development quotient was 67, as determined using the Tanaka-Binet Scale of Psychological Development; this

Author's personal copy

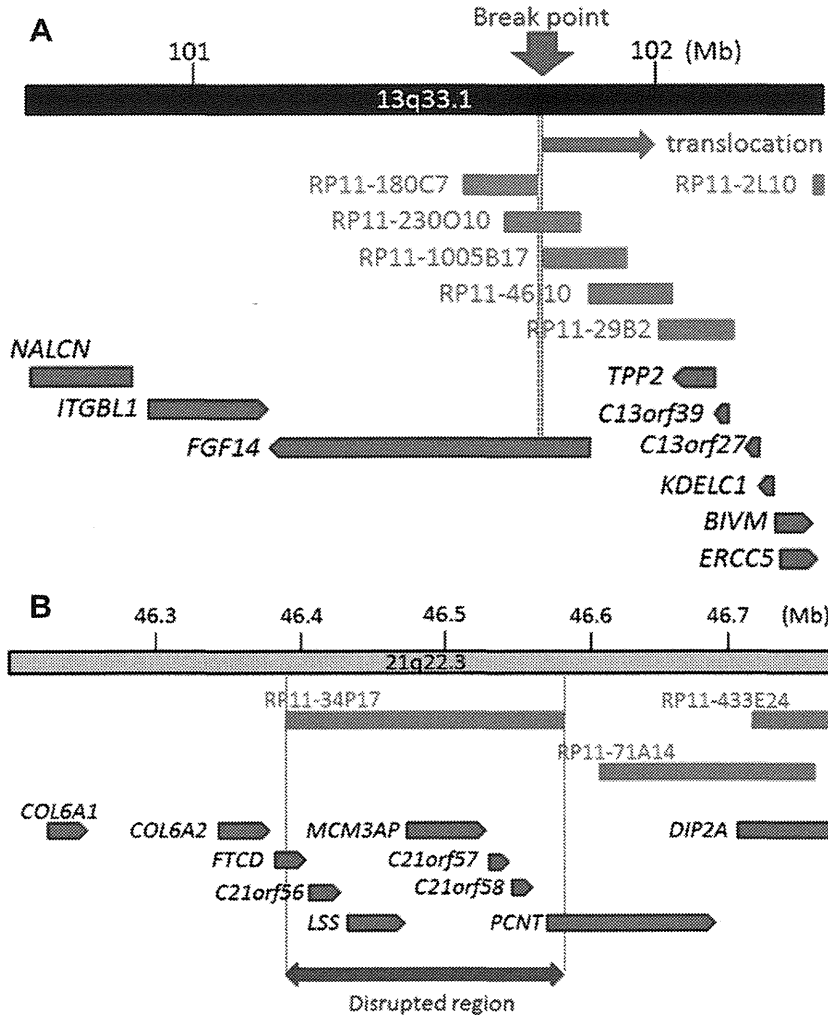

Fig. 2. Physical maps around the breakpoints of translocation. (A) Although RP11-230O10 is disrupted, RP11-180C7 and RP11-1005B17 are not disrupted. This indicates that the break point of this region is narrowed into 10-kb region covering *FGF14*. (B) The disrupted BAC clone, RP11-34P17, includes seven known genes. However, these seven genes do not show any functional relevance to the patient's neurological findings. Rectangles and pentagons indicate the locations of the BAC clones and the known genes, respectively. Italic symbols indicate the name of the genes.

value indicated mild mental retardation [3]. He graduated from a special educational school and is now 19 years old. Conventional chromosomal analysis detected the presence of a reciprocal translocation with the karyotype 46,XY,t(13;21)(q32;q22.3). Since his parents showed normal karyotypes, the patient's translocation was considered as a de novo translocation.

Fluorescent *in situ* hybridization (FISH) analysis was performed to investigate the breakpoints of the translocation, according to a previously described method [4]. BAC clones used as the probes were selected from the suspected breakpoints using UCSC genome browser (http://www.genome.ucsc.edu) (Table 1). Although one of the signals of RP11-230O10 was split into chromosome 21 (Fig. 1A), the neighboring two BAC clones were not disrupted. Thus, the breakpoint was narrowed into 10-kb region of chr13:101,742,909–101,752,504 which disrupted *FGF14* (Fig. 2A). Similarly, the breakpoint on chromosome 21 within the 21q22.3 band was determined on the region of RP11-34P17 (Fig. 1B), which included seven known genes with no functional relevance to the patient's neurological findings (Fig. 2B). From these evidences, we concluded that the phenotype observed in this patient could be attributable to the breakage of *FGF14*.

The myofibrillogenesis regulator 1 gene (*MR-1*) is known to be responsible for PNKD [5]; therefore, we analyzed the nucleotide sequences of *MR-1* and *FGF14* for this patient by using the standard polymerase chain reaction (PCR)-direct sequencing method with primers designed using web-based PRIMER 3 software (Supplementary Table S1), and there was no nucleotide alteration in this patient. Then, we participated in the cohort study using DNA samples obtained from the other six children (two males and four females from five families, age 3–16 years old) who were diagnosed as

Author's personal copy

having PNKD based on the reported description [6]. The result showed no nucleotide alteration in *MR-1* and *FGF14*.

3. Discussion

Our patient started exhibiting episodic involuntary movements when he was 8 months old. Because his consciousness was not disturbed, these movements were considered as nonepileptic paroxysmal movements. Despite the lack of a family history of PNKD, we considered his clinical diagnosis as PNKD, which is an autosomal dominant hereditary movement disorder exhibiting involuntary movements, including chorea, ballismus, and dystonia with the onset age usually 1–12 years [7].

In this patient, a de novo reciprocal chromosomal translocation between chromosomes 13 and 20 was identified, and detailed cytogenetic analyses confirmed a disruption in *FGF14*, which is recognized as the cause of SCA27, since two *FGF14* mutations have been reported in large SCA families [8,9]. Therefore, the genetic diagnosis of this patient was confirmed as SCA27 not PNKD. It was hard to diagnose him as SCA27 before the genetic diagnosis, because SCAs generally show wide spectrum of clinical phenotypes and because this patient was a sporadic case and there was no family history [1].

Previous study reported a daughter and her mother who had the identical reciprocal translocation between chromosomes 5 and 13 [10]. In the family, the breakpoint on chromosome 13 disrupted *FGF14* same as our patient. Although the mother exhibited mental impairment and pes cavus, gait ataxia was observed only when she closed her eyes; this indicated very mild cerebellar involvement. In contrast, the daughter began to exhibit cerebellar dysfunctions with gait ataxia and tremor since the first year of life. She also exhibited dyskinetic jerky movements. These clinical features are similar to those observed in our patient. This evidence suggests that disruption or loss-of-function mutations in *FGF14* may be responsible for SCA27 but the disease penetrance would be less than 100%. In addition, phenotypic overlapping of PNKD and SCA27 is observed in this family and our patient.

PNKD exhibits genetic heterogeneity, because approximately 60% of patients with PNKD exhibit *MR-1* mutations [7], but the causative factors have not yet been identified for the remaining 40% of patients with PNKD. Therefore, we hypothesized that *FGF14* may be responsible for the remaining 40% of patients with PNKD and that this may be the reason of phenotypic overlapping of PNKD and SCA27. Based on this hypothesis, we analyzed the nucleotide sequences of *MR-1* and *FGF14* in six patients with PNKD, but there were no mutations. This result may be attributable to the small study population used in this study. Therefore, further studies are required to prove our hypothesis.

Conflict of interest

The all authors declare no conflict of interest.

Acknowledgment

Dr. Shimojima thanks Hayashi Memorial Foundation for Female Natural Scientists for the grant aid support.

Appendix A. Supplementary data

Supplementary data associated with this article can be found, in the online version, at doi:10.1016/j.braindev.2011.04.014.

References

[1] Manto MU. The wide spectrum of spinocerebellar ataxias (SCAs). Cerebellum 2005;4:2–6.
[2] Soong BW, Paulson HL. Spinocerebellar ataxias: an update. Curr Opin Neurol 2007;20:438–46.
[3] Koeda T, Takeshita K. Visuo-perceptual impairment and cerebral lesions in spastic diplegia with preterm birth. Brain Dev 1992;14:239–44.
[4] Shimojima K, Sugiura C, Takahashi H, Ikegami M, Takahashi Y, Ohno K, et al. Genomic copy number variations at 17p13.3 and epileptogenesis. Epilepsy Res 2010;89:303–9.
[5] Rainier S, Thomas D, Tokarz D, Ming L, Bui M, Plein E, et al. Myofibrillogenesis regulator 1 gene mutations cause paroxysmal dystonic choreoathetosis. Arch Neurol 2004;61:1025–9.
[6] van Rootselaar AF, van Westrum SS, Velis DN, Tijssen MA. The paroxysmal dyskinesias. Pract Neurol 2009;9:102–9.
[7] Bruno MK, Lee HY, Auburger GW, Friedman A, Nielsen JE, Lang AE, et al. Genotype–phenotype correlation of paroxysmal non-kinesigenic dyskinesia. Neurology 2007;68:1782–9.
[8] van Swieten JC, Brusse E, de Graaf BM, Krieger E, van de Graaf R, de Koning I, et al. A mutation in the fibroblast growth factor 14 gene is associated with autosomal dominant cerebellar ataxia [corrected]. Am J Hum Genet 2003;72:191–9.
[9] Dalski A, Atici J, Kreuz FR, Hellenbroich Y, Schwinger E, Zuhlke C. Mutation analysis in the fibroblast growth factor 14 gene: frameshift mutation and polymorphisms in patients with inherited ataxias. Eur J Hum Genet 2005;13:118–20.
[10] Misceo D, Fannemel M, Baroy T, Roberto R, Tvedt B, Jaeger T, et al. SCA27 caused by a chromosome translocation: further delineation of the phenotype. Neurogenetics 2009;10:371–4.

CLINICAL REPORT

AMERICAN JOURNAL OF medical genetics PART A

De Novo Microdeletion of 5q14.3 Excluding *MEF2C* in a Patient With Infantile Spasms, Microcephaly, and Agenesis of the Corpus Callosum

Keiko Shimojima,[1] Akihisa Okumura,[2] Harushi Mori,[3] Shinpei Abe,[2] Mitsuru Ikeno,[2] Toshiaki Shimizu,[2] and Toshiyuki Yamamoto[1]*

[1]Tokyo Women's Medical University Institute for Integrated Medical Sciences, Tokyo, Japan

[2]Department of Pediatrics, Juntendo University School of Medicine, Tokyo, Japan

[3]Department of Radiology, Graduate School and Faculty of Medicine, The University of Tokyo, Tokyo, Japan

Manuscript Received: 14 November 2011; Manuscript Accepted: 25 April 2012

The 5q14.3 microdeletion syndrome has recently been recognized as a clinical entity manifesting as severe intellectual disability, epilepsy, and brain malformations. Analysis of the shortest region of overlap among patients with this syndrome and subsequent identification of nucleotide alterations in the coding region of myocyte enhancer factor 2C gene (*MEF2C*) have suggested *MEF2C* as the gene responsible for the 5q14.3 microdeletion syndrome. We identified a de novo 3.4-Mb deletion of 5q14.3 in a patient with infantile spasms, microcephaly, and brain malformation. The deleted region in the present patient was positional toward the centromere, and *MEF2C* was not included in the deleted region. However the neurological and dysmorphic features of the present patient resembled those of patients with the 5q14.3 microdeletion syndrome. We consider that a positional effect is the likely explanation for this evidence. To study the precise mechanism of this positional effect, further information is required on patients showing atypical deletions neighboring *MEF2C*. © 2012 Wiley Periodicals, Inc.

Key words: 5q14.3 deletion; *MEF2C*; infantile spasms; agenesis of the corpus callosum

How to Cite this Article:
Shimojima K, Okumura A, Mori H, Abe S, Ikeno M, Shimizu T, Yamamoto T. 2012. De novo microdeletion of 5q14.3 excluding *MEF2C* in a patient with infantile Spasms, microcephaly, and agenesis of the corpus callosum.
Am J Med Genet Part A 158A:2272–2276.

INTRODUCTION

The 5q14.3 microdeletion syndrome has recently been recognized as a clinical entity manifesting with severe intellectual disability, epilepsy, and brain malformations [Cardoso et al., 2009; Zweier et al., 2010]. Previous studies have reported 22 patients with 5q14.3 deletions [Cardoso et al., 2009; Engels et al., 2009; Sobreira et al., 2009; Berland and Houge, 2010; Le Meur et al., 2010; Marashly et al., 2010; Novara et al., 2010; Nowakowska et al., 2010; Zweier et al., 2010]. The myocyte enhancer factor 2C gene (*MEF2C*) is located on the shortest region of overlap among them. In addition de novo mutations in the coding sequences of *MEF2C* have been identified in patients with similar findings to patients who exhibit common phenotypic features of severe intellectual disability, stereotyped behaviors, poor eye contact, absent speech, and epilepsy [Zweier et al., 2010]. Thus, *MEF2C* is currently recognized as the main gene responsible for the 5q14.3 microdeletion syndrome.

Here, we present a patient with the 5q14.3 microdeletion syndrome manifesting with infantile spasms, microcephaly, and brain malformation. However, the deleted region in this patient did not include *MEF2C*. The genotype–phenotype correlation in this patient will be discussed in this report.

CLINICAL REPORT

A 1-year-8-month-old boy was born at term following an uneventful pregnancy as the first child from healthy non-related parents. His birth length was 48 cm (25–50th centile), birth weight was

Additional supporting information may be found in the online version of this article.

Grant sponsor: Japan Ministry of Education, Science, Sports and Culture; Grant numbers: 21591334, 22890199.

*Correspondence to:
Toshiyuki Yamamoto, MD, PhD, Tokyo Women's Medical University Institute for Integrated Medical Sciences, 8-1 Kawada-cho, Shinjuku-ward, Tokyo 162-8666, Japan. E-mail: yamamoto.toshiyuki@twmu.ac.jp

Article first published online in Wiley Online Library (wileyonlinelibrary.com): 27 July 2012
DOI 10.1002/ajmg.a.35490

© 2012 Wiley Periodicals, Inc.

3,100 g (50–75th centile), and head circumference was 31.0 cm (<3rd centile). He showed remarkable generalized hypotonia at birth. He exhibited feeding difficulty and respiratory distress due to a combination of dysphagia and narrowing of the upper airways. His respiratory distress and subsequent opisthotonic posture gradually caused bad temper, which exacerbated the truncal hypertonia. His developmental milestone was delayed with head control achieved at 7 months, and visual fixation and social smile at 1 year.

He experienced epileptic seizures at 4 months of age, which were characterized by spasms in clusters, sudden drops of the head, abductions of the arms, and upward rolling of the eyes for a few seconds followed by crying. Electroencephalography (EEG) indicated atypical hypsarrhythmia. At 5 months of age, adrenocorticotrophic hormone (ACTH) therapy was initiated, and the epileptic seizures disappeared. Currently, his seizures are well controlled without medication.

Brain magnetic resonance imaging (MRI) performed at 1 year and 1 month of age showed reduced volume of the frontal lobe, hypoplastic corpus callosum, and dilatation of the lateral cerebral ventricles (Fig. 1). The volume of white matter was markedly reduced, particularly in the frontal and anterior temporal lobes. No delay in myelination was observed. The dilatation of the lateral ventricles was remarkable, particularly in the occipital and inferior horns and showed colpocephalic appearance. Periventricular heterotopia, which was previously reported by Cardoso et al. [2009] was not observed (Fig. 1). Severe dysgenesis of the corpus callosum was evident, but the cingulate gyrus was preserved. Longitudinal fibers, such as the bundle of Probst, were observed along the mesial

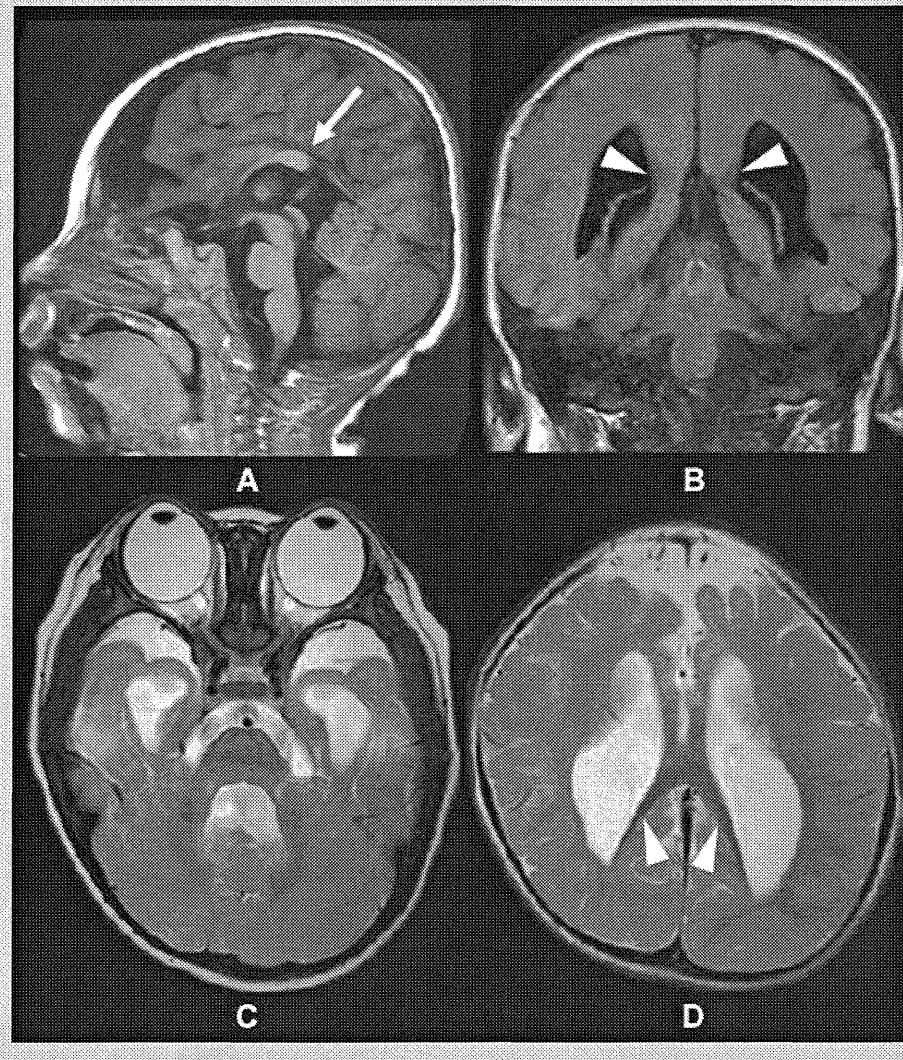

FIG. 1. MRI findings of the patient. A: Sagittal T1-weighted image. The corpus callosum is markedly hypoplastic (arrow), whereas the cingulate gyrus is preserved. The volume of the brainstem is proportionally reduced compared to that of the cerebral white matter. B: Coronal fluid-attenuated inversion-recovery image. Longitudinal fibers, such as the bundle of Probst, are detected in the mesial margins of the lateral ventricles (arrow heads). C, D: Axial T2-weighted images. A marked dilatation of the lateral ventricles is noted along with a marked reduction in the volume of cerebral white matter, particularly in the frontal and anterior temporal lobes. Longitudinal fibers, such as the bundle of Probst, are present in the mesial wall of the posterior part of the lateral ventricles (D, arrow heads).

wall of the posterior part of the lateral ventricles. The anterior commissure was normal, and the ventral part of the fornix was hyperplastic. The volume of the brainstem was proportionally reduced according to that of the cerebral matter. The upper cerebellar peduncles were hypoplastic, whereas the cerebellum was preserved.

At present, the patient's height was 73.1 cm (<3rd centile) and weight was 7.56 kg (<3rd centile). He has microcephaly with a head circumference of 41.0 cm (<3rd centile). Although he can follow things with his eyes and control his neck movement, he cannot sit nor roll over and does not have meaningful speech. He shows distinctive facial findings, including flat occiput, hypertelorism, depressed nasal bridge, small nose, low-set ears, micrognathia, short tapering fingers, and single transverse palmar creases in both hands (Supplemental eTable SI—See Supporting Information online). Deep tendon reflexes are hyperactive. The range of motion (ROM) of his arms and legs are restricted due to generalized hypertonia but no joint contracture is observed. Pathological reflexes, including Babinski reflexes, are not remarkable. These findings indicate spastic quadriplegia, although he showed hypotonia in his early infantile period. His generalized hypertonia had gradually become prominent during early infancy.

GENETIC ANALYSES

The findings of the conventional cytogenetic analysis with GTG-banding showed normal male karyotype with 46,XY. We then performed a microarray-based comparative genomic hybridization (aCGH) analysis using Agilent 44K oligonucleotide microarray (Agilent Technologies, Santa Clara, CA) according to a previously described method [Shimojima et al., 2009]. Through this analysis, we identified the loss of a genomic copy number at the 5q14.3 region with the size of 3.4-Mb indicating arr 5q14.3(83,468,682–86,939,957) × 1 (referring Build 2006) (Fig. 2A). The identified aberration region included six genes, EGF-like repeats and discoidin I-like gene (*EDIL3*), homo sapiens cDNA, FLJ98222 (*NBPF22F*), cytochrome

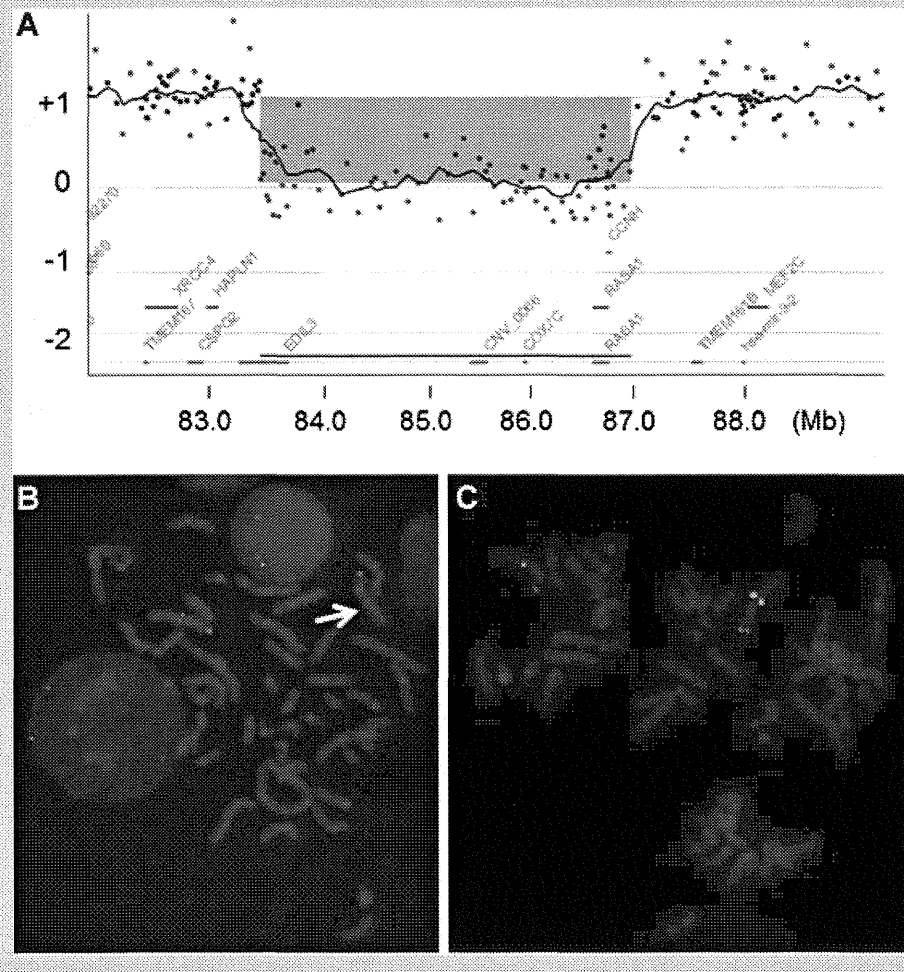

FIG. 2. Results of the molecular and cytogenetic analyses. A: A 3.4-Mb deletion of 5q14.3 identified in the present patient is shown by Gene View of Agilent Genomic Workbench (Agilent Technologies). The horizontal axis indicates the physical position of 5q14.3, and the vertical axis indicates gain or loss of genome copy number. The aberration area is indicated by a blue rectangle. B, C: FISH analyses using green signals of RP11-111M24 covering *RASA1* (B) and RP11-117A24 covering *MEF2C* (C) indicate a deletion of the *RASA1* region (arrow) but no deletion of *MEF2C*. Red signal for RP11-94J21 on 5p15.33 is used as the marker for chromosome 5.

c oxidase subunit VIIc precursor (*COX7C*), cDNA FLJ13355 fis, clone PLACE1000048 (*FLJ11292*), RAS p21 protein activator 1 gene (*RASA1*), and cyclin H gene (*CCNH*) (Supplemental eTable SII—See Supporting Information online). However, *MEF2C* was not included in the deletion region (Fig. 2A). The identified aberration was validated through fluorescent in-situ hybridization (FISH) as previously described [Shimojima et al., 2009] using BAC clones RP11-111M24 on 5q14.3 covering *RASA1* (Fig. 2B) and RP11-117A24 on 5q14.3 covering *MEF2C* (Fig. 2C). RP11-94J21 on 5p15.33 was used as a marker for chromosome 5. FISH reconfirmed the result of aCGH, and the final karyotype was determined to be ish del(5)(q14.3q14.3)(RP11-94J21+,RP11-111M24−,RP11-117A24+). Parental FISH analyses showed no 5q14.3 deletion in either parent, indicating a de novo occurrence (data not shown).

Expression levels of *MEF2C* and *CCNH* were analyzed by real-time PCR method using SYBR Green system as described elsewhere [Filges et al., 2011]. Total RNA extracted from immortalized lymphoblasts from the present patient and a normal control individual were used for templates. The primers used for this examination were listed in Supplemental eTable SIII (See Supporting Information online). Because *MEF2C* and *CCNH* have two different isoforms, expression levels of both isoforms were measured in three independent replicates on MX3000P (Agilent Technologies). Expression level of glyceraldehyde-3-phosphate dehydrogenase gene (*GAPDH*) was used for the internal control. Obtained data were evaluated by the Delta Delta Ct method [Filges et al., 2011]. After evaluation, the expression ratio (patient versus normal control) was calculated in each of the three examinations and the averaged data of three examinations were shown in Supplemental eFigure S1 (See Supporting Information online). Although both of the isoforms 1 and 2 of *MEF2C* did not show any significant decreases, significantly decreased expressions of *CCNH* were clearly shown in both of the isoforms 1 and 2 (Supplemental eFigure S1—See Supporting Information online).

DISCUSSION

The present patient showed neurological manifestations with severe hypotonia and subsequent feeding difficulty in his early infancy. His developmental delay was remarkable; he could not sit alone nor turn over by himself at his age of 1 year and 8 months. Although he is now seizure free, he suffered infantile spasms at the age of 4 months. He also showed dysmorphic findings including microcephaly, depressed nasal bridge, small nose, low-set ears, and micrognathia. All of these manifestations are associated with the 5q14.3 microdeletion syndrome [Zweier et al., 2010].

Brain MRI on this patient indicated severe findings (Fig. 1). The most striking MRI finding was the hypoplastic corpus callosum. Colpocephaly with marked dilatations of the lateral venricles and a marked reduction in volume of white matter would be the consequence of the hypoplastic corpus callosum. Dilatation of the fourth ventricle was also noted, which may be associated with a mildly hypoplastic brain stem. Another characteristic of this patient was the reduced volume of the frontal lobe resulting in dilatation of extracerebral space around the frontal lobe.

Although not all dysmorphic, neurological, and radiological findings of this patient are common in the 5q14.3 microdeletion syndrome, many are frequently observed in these patients [Zweier

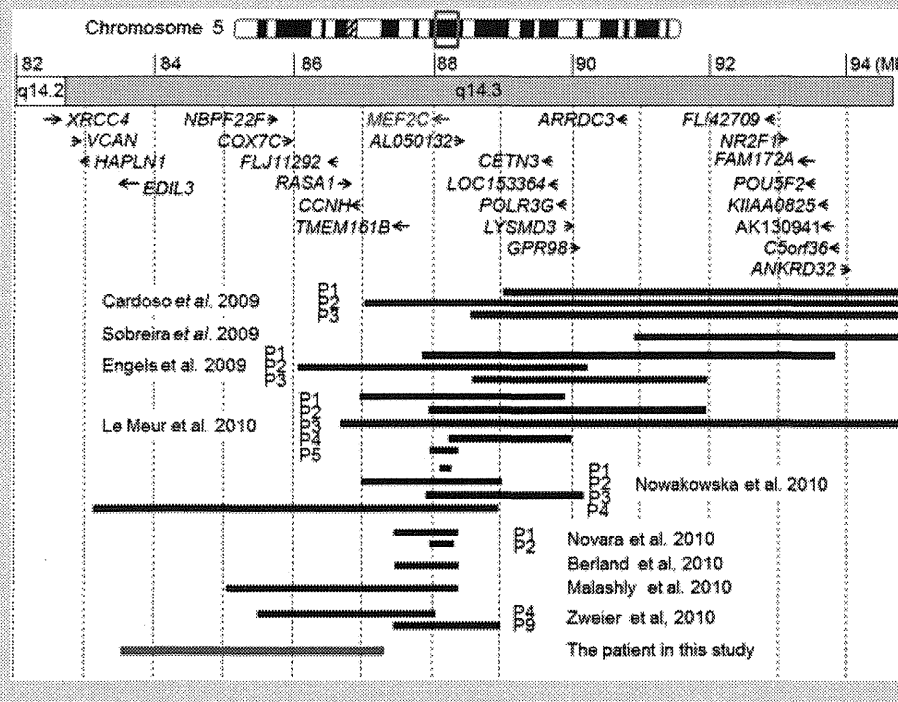

FIG. 3. The physical map around 5q14.3 depicted of the reported deletions. Black arrows represent the direction and the length of each gene. The extents of the previously reported deletions are shown by black bars.

et al., 2010] (Supplemental eTable SI—See Supporting Information online). Therefore, clear evidence for rejecting the 5q14.3 microdeletion syndrome diagnosis on the present patient could not be found. However, the deleted region of the present patient did not include *MEF2C*, the main gene hypothesized to be responsible for the 5q14.3 microdeletion syndrome [Zweier et al., 2010]. Among 22 previously reported patients with 5q14.3 deletions, four patients showed deletions in which only upstream regions of *MEF2C* were included but the coding region of *MEF2C* was not included (Fig. 3) [Cardoso et al., 2009; Engels et al., 2009]. Recently, Saitsu et al. [2011] reported a patient with intellectual disability and early-onset epileptic encephalopathy derived from a de novo reciprocal chromosomal translocation with a disrupted upstream region of *MEF2C*. The authors speculated that chromosomal translocation impaired the proper regulation of *MEF2C* expression in the developing brain [Saitsu et al., 2011]. Compared to that observation, the present patient showed a deletion on the downstream region of *MEF2C*. To confirm the functional relevance of the genes around this region, we analyzed the expression level of *MEF2C* and *CCNH* in the lymphoblast cells derived from the patient. The results showed decreased expression of *CCNH* in the deleted region; however, decreased expression of *MEF2C* was not observed. Because the case reported by Saitsu et al. [2011] also did not show a significant decrease in *MEF2C* expression, our result does not negate the correlation of *MEF2C* in neurological manifestations. This is a limitation of the use of lymphoblast cells for investigation of neurological disorders.

We analyzed the literature and in-silico data and determined that none of the six genes in the deleted region of the present patient showed direct correlation with the phenotypic features of this patient (Supplementary eTable SII—See Supporting Information online). Although the deleted region of the present patient shifted toward the centromere, and *MEF2C* was not included, the neurological and dysmorphic features of the present patient resembled those of the 5q14.3 microdeletion syndrome patients [Zweier et al., 2010]. We consider that a positional effect is the only potential explanation for this evidence [Kleinjan and van Heyningen, 1998; Kleinjan and van Heyningen, 2005]. To study the precise mechanism of this positional effect, further information is required on patients showing atypical deletions neighboring *MEF2C*.

ACKNOWLEDGMENTS

We thank the patient and his parents for their gracious participation and support. This work was supported by Grant-in-Aid for Scientific Research (C) 21591334 (T.Y.) and Grant-in-Aid for Research Activity Start-up 22890199 (K.S.) from the Japan Ministry of Education, Science, Sports and Culture.

REFERENCES

Berland S, Houge G. 2010. Late-onset gain of skills and peculiar jugular pit in an 11-year-old girl with 5q14.3 microdeletion including MEF2C. Clin Dysmorphol 19:222–224.

Cardoso C, Boys A, Parrini E, Mignon-Ravix C, McMahon JM, Khantane S, Bertini E, Pallesi E, Missirian C, Zuffardi O, Novara F, Villard L, Giglio S, Chabrol B, Slater HR, Moncla A, Scheffer IE, Guerrini R. 2009. Periventricular heterotopia, mental retardation, and epilepsy associated with 5q14.3-q15 deletion. Neurology 72:784–792.

Engels H, Wohlleber E, Zink A, Hoyer J, Ludwig KU, Brockschmidt FF, Wieczorek D, Moog U, Hellmann-Mersch B, Weber RG, Willatt L, Kreiss-Nachtsheim M, Firth HV, Rauch A. 2009. A novel microdeletion syndrome involving 5q14.3-q15: Clinical and molecular cytogenetic characterization of three patients. Eur J Hum Genet 17:1592–1599.

Filges I, Shimojima K, Okamoto N, Rothlisberger B, Weber P, Huber AR, Nishizawa T, Datta AN, Miny P, Yamamoto T. 2011. Reduced expression by SETBP1 haploinsufficiency causes developmental and expressive language delay indicating a phenotype distinct from Schinzel-Giedion syndrome. J Med Genet 48:117–122.

Kleinjan DA, van Heyningen V. 2005. Long-range control of gene expression: Emerging mechanisms and disruption in disease. Am J Hum Genet 76:8–32.

Kleinjan DJ, van Heyningen V. 1998. Position effect in human genetic disease. Hum Mol Genet 7:1611–1618.

Le Meur N, Holder-Espinasse M, Jaillard S, Goldenberg A, Joriot S, Amati-Bonneau P, Guichet A, Barth M, Charollais A, Journel H, Auvin S, Boucher C, Kerckaert JP, David V, Manouvrier-Hanu S, Saugier-Veber P, Frebourg T, Dubourg C, Andrieux J, Bonneau D. 2010. MEF2C haploinsufficiency caused by either microdeletion of the 5q14.3 region or mutation is responsible for severe mental retardation with stereotypic movements, epilepsy and/or cerebral malformations. J Med Genet 47: 22–29.

Marashly A, Riel-Romero RM, Ursin S, Ghawi H. 2010. Infantile spasms associated with 5q14.3 deletion. J La State Med Soc 162:223–226.

Novara F, Beri S, Giorda R, Ortibus E, Nageshappa S, Darra F, Dalla Bernardina B, Zuffardi O, Van Esch H. 2010. Refining the phenotype associated with MEF2C haploinsufficiency. Clin Genet 78:471–477.

Nowakowska BA, Obersztyn E, Szymanska K, Bekiesinska-Figatowska M, Xia Z, Ricks CB, Bocian E, Stockton DW, Szczaluba K, Nawara M, Patel A, Scott DA, Cheung SW, Bohan TP, Stankiewicz P. 2010. Severe mental retardation, seizures, and hypotonia due to deletions of MEF2C. Am J Med Genet B Neuropsychiatr Genet 153B:1042–1051.

Saitsu H, Igarashi N, Kato M, Okada I, Kosho T, Shimokawa O, Sasaki Y, Nishiyama K, Tsurusaki Y, Doi H, Miyake N, Harada N, Hayasaka K, Matasumoto N. 2011. De novo 5q14.3 translocation 121.5-kb upstream of MEF2C in a patient with severe intellectual disability and early-onset epileptic encephalopathy. Am J Med Genet Part A 155A: 2879–2884.

Shimojima K, Komoike Y, Tohyama J, Takahashi S, Paez MT, Nakagawa E, Goto Y, Ohno K, Ohtsu M, Oguni H, Osawa M, Higashinakagawa T, Yamamoto T. 2009. TULIP1 (RALGAPA1) haploinsufficiency with brain development delay. Genomics 94:414–422.

Sobreira N, Walsh MF, Batista D, Wang T. 2009. Interstitial deletion 5q14.3-q21 associated with iris coloboma, hearing loss, dental anomaly, moderate intellectual disability, and attention deficit and hyperactivity disorder. Am J Med Genet Part A 149A:2581–2583.

Zweier M, Gregor A, Zweier C, Engels H, Sticht H, Wohlleber E, Bijlsma EK, Holder SE, Zenker M, Rossier E, Grasshoff U, Johnson DS, Robertson L, Firth HV, Ekici AB, Reis A, Rauch A. 2010. Mutations in MEF2C from the 5q14.3q15 microdeletion syndrome region are a frequent cause of severe mental retardation and diminish MECP2 and CDKL5 expression. Hum Mutat 31:722–733.

脳と発達 2012；44：450―454

＝原著論文＝

本邦における先天性筋無力症候群の臨床的特徴

苛原 香[1] 小牧 宏文[1] 本田 涼子[1] 奥村 彰久[2] 白石 一浩[3]
小林 悠[4] 東 慶輝[5] 中田 智彦[5] 大矢 寧[6] 佐々木征行[1]

要旨

【目的】先天性筋無力症候群（congenital myasthenic syndrome；CMS）の特徴を明らかにする．

【方法】CMSと診断した5例の臨床経過，診察所見，電気生理学的所見などを後方視的に検討した．

【結果】4例が乳児早期に筋力低下と運動発達遅滞，1例は3歳時に運動不耐で発症した．幼児期以降に1日単位で変動または数日間持続する筋力低下を全例で認めたのが特徴的で，日内変動を示したのは1例のみであった．反復神経刺激では，遠位の運動神経では減衰を認めない例があった．塩酸エドロフォニウム試験では，眼瞼下垂を示した3例全例で改善を認めなかった．全例で薬物治療による改善を示した．

【結論】CMSはていねいな診察と電気生理検査により診断可能で薬物治療が行える疾患である．

見出し語 先天性筋無力症候群，筋力変動，塩酸エドロフォニウム試験，反復神経刺激

はじめに

先天性筋無力症候群（congenital myasthenic syndrome；CMS）は，神経筋接合部の先天的分子欠損により全身の筋力低下，易疲労性を呈し[1)2)]，生後1年以内に発症することが多い[3)]稀な疾患である．多くは近位筋優位の筋力低下に加えて外眼筋障害，眼瞼下垂を呈し，自己免疫性の重症筋無力症や先天性ミオパチーと似た臨床像を呈する[4)5)]が，軽度の筋力低下のみを呈し，眼瞼下垂を欠く例[5)]や成人発症例[2)3)6)]があるなどの理由から診断に長期間を要する例が少なくない[2)7)]．欧米を中心に，すでに200家系以上のCMSが報告されている[8)]が，本邦での報告は検索する限り4例[9)～12)]のみであり，確定診断がなされていない例が多い可能性がある．我々は日本人小児のCMS 5例の臨床情報を後方視的に解析し，他疾患との鑑別となる症状，電気生理学的特徴などについて検討した．

第53回日本小児神経学会総会推薦論文

[1]国立精神・神経医療研究センター病院小児神経科
[2]順天堂大学医学部小児科・思春期科
[3]国立病院機構宇多野病院小児科
[4]国立病院機構西新潟中央病院小児科
[5]名古屋大学大学院医学系研究科・神経遺伝情報学
[6]国立精神・神経医療研究センター病院神経内科

連絡先 〒187-8551 小平市小川東町4-1-1
国立精神・神経医療研究センター病院小児神経科
（小牧宏文）
E-mail：komakih(a)ncnp.go.jp

（受付日：2011. 6. 20，受理日：2011. 11. 29）

Ⅰ 対象・方法

発症時期，臨床症状，反復神経刺激（repetitive nerve stimulation；RNS）減衰からCMSを疑い，遺伝子解析にて病因と考えられる変異が判明した5例を対象とし，診療録に基づいて，臨床的特徴として，妊娠経過，発症時期，発症時の臨床症状，家族歴，その後の発達，経過，現在の状態，および電気生理学的特徴について検討した．遺伝子解析は文書による保護者の同意を得て行った．RNSは正中神経2例（左側1例，右側1例），尺骨神経3例（左側2例，右側1例），腓骨神経3例（両側1例，左側2例），副神経3例（両側2例，左側1例）を1，3，5，10 Hzの刺激頻度で評価した（重複含む）．第1反応と最小振幅のcompound muscle action potential（以下CMAP）を比較してその差が第1反応の10%以上あれば減衰現象陽性とした．塩酸エドロフォニウム試験は，眼瞼下垂の変化の他に投与後のCMAP減衰率の改善，または階段昇降の所要時間の短縮を認めた例を陽性，これらが不変であった例を陰性，症状が悪化した例を悪化とした．自己抗体は抗アセチルコリン受容体（acetylcholine receptor 以下AChR）抗体，抗muscle specific kinase（以下MuSK）抗体を検索した．

Ⅱ 結 果

1. 臨床的特徴（表1）

症例は男児4例，女児1例で評価時の年齢は6～19歳であった．新生児期発症3例（症例1～3），乳児期発症1例（症例4），幼児期発症1例（症例5）で，4例が生後1年以内に発症した．妊娠経過中の異常は全例認めなかった．症例1では生直後から自発呼吸が確立せず，気管切開と人工呼吸管理を行い，現在まで継続している．初発症状は4例（症例

Presented by Medical*Online

表 1　各症例の臨床像

症例		1	2	3	4	5
性別		M	M	M	F	M
評価時年齢		9 歳 3 カ月	12 歳 2 カ月	19 歳	6 歳 10 カ月	6 歳 11 カ月
発症年齢		0 カ月	0 カ月	0 カ月	乳児期	3 歳
初発症状		筋力低下 筋緊張低下 呼吸不全	筋緊張低下 哺乳微弱 体重増加不良	眼瞼下垂 哺乳力低下	運動発達遅滞	運動不耐
初診		0 カ月	6 カ月	9 歳	5 歳 3 カ月	5 歳
初診時主訴		同上	運動発達遅滞 呼吸不全	眼瞼下垂	感染 / 喘息発作後の 一過性筋力低下 易疲労性	同上
運動発達		頸定 2 歳 独歩 4 歳 8 カ月	頸定 6 カ月 独歩 2 歳	頸定 8 カ月 独歩 1 歳 7 カ月	頸定 7 カ月 独歩 1 歳 4 カ月	頸定 3 カ月 独歩 1 歳 6 カ月
精神発達		境界域	正常	正常	正常	正常
眼瞼下垂		あり	あり	あり	なし	なし
眼球運動制限		全方向	外転	なし	なし	なし
筋緊張低下		頸部	四肢，体幹	なし	四肢，体幹	なし
徒手筋力テスト		頸部 2，体幹 3，四肢 4	頸部・体幹 2，四肢 4	頸部・上肢 4	四肢 4	頸部 4
筋力変動	日内変動	なし	なし	あり	なし	なし
	日によって程度が異なる筋力低下	誘因なく，歩行できない日，平地歩行のみ可能な日，平地歩行に加えて階段昇降が可能な日があり，日によって調子が異なる	誘因なく，階段昇降が可能な日と不可能な日があり，日によって調子が異なる	なし	なし	誘因なく，15 分の歩行で動揺性歩行を呈する日，2 時間の歩行で動揺性歩行を呈する日，階段昇降をしても無症状の日があり，日によって調子が異なる
	数日以上続く筋力低下	疲労後から歩行距離の短縮が数日間続く	なし	運動負荷後に疲労感と軽度の筋力低下が数日間続く	喘息発作 1 週間後に起立困難が約 1 週間続く	なし
呼吸不全		気管切開 人工呼吸器管理 4 歳から夜間のみ使用	感冒時に反復 11 歳時夜間 NIV 導入	12 歳時夜間 NIV 導入	なし	なし
遺伝子変異		*DOK7* c.190G>A, p.R64R/ c.653-1G>C	*COLQ* c.1339G>C, p.D447H (homozygote)	*COLQ* c.C679T, p.R227X/ c.T965A, p.V322D	*CHRNE* c.790A>C, p.T264P (heterozygote)	*COLQ* c.1331G>A, p.C444Y/ c.1354C>T, p.R452C
診断時の年齢		10 歳	12 歳	19 歳	7 歳	7 歳
内服薬（1 日量）/ 体重		ephedrine hydrochloride 20 mg, 3,4-DAP 20 mg/21 kg	ephedrine hydrochloride 100 mg/40 kg	ephedrine hydrochloride 100 mg/50 kg	pyridostigmine bromide 90 mg, 3,4-DAP 30 mg, ephedrine hydrochloride 25 mg/32 kg	ephedrine hydrochloride 75 mg/25 kg
治療後の変化		両上肢の挙上時間延長 臥位から立位への体位変換の所要時間短縮	歩行距離延長	易疲労性改善	階段昇降時間短縮	易疲労性改善

M：male，F：female
NIV：non-invasive ventilation，3,4-DAP：3,4-Diaminopyridine

1 ～ 4）で明らかな筋緊張低下，筋力低下を認めフロッピーインファントと言える状態であった．乳児期後期以降は運動発達を認めるようになり，3 例が 1 歳 7 カ月までに，遅い例（症例 1）でも 4 歳時に独歩を獲得した．幼児期発症の 1 例（症例 5）は 3 歳時に長距離歩行後の動揺性歩行で発症した．家族歴は症例 5 のみに認め，父方祖母が重症筋無力症と診断されていたが，詳細な情報は得られなかった．これらの臨床的特徴は従来の報告に合致していた．

評価時には全身の筋力低下を 2 例，頸部・四肢に限局した筋力低下を 3 例に認めた．最も特徴的な症状は筋力の変動であり，全例に認めた．筋力変動は夕方に増悪する筋力低下を呈する日内変動を 1 例，日によって程度の異なる筋力低下を呈する変動を 3 例，筋力低下が数日～数カ月単位で持続する長期変動を 3 例に認めた（症例の重複あり）．日内変動のみを呈した例はなかった．以下に日によって程度の異なる筋力変動について具体的に述べる．症例 1 は日によって歩行不能な日，平地歩行が可能な日，平地歩行に加えて 10 段程度の階段昇降が可能な日があった．症例 2 は症例 1 ほどの大きな変

Presented by Medical*Online

表2 反復神経刺激検査結果・塩酸エドロフォニウム試験・筋生検結果

症例			1	2	3	4	5
RNS 減衰率	正中神経		減衰なし	NE	NE	60.2%	NE
	尺骨神経		NE	減衰なし /82%（強収縮負荷後）	52%	68.2%	NE
	腓骨神経		NE	55.3%	NE	23.4%	減衰なし
	副神経		79%	78.6%	NE	NE	33.9%
塩酸エドロフォニウム試験	結果		陽性	悪化	陰性	陽性	陽性
	判定根拠	全身症状	変化なし	投与後に呼吸不全	変化なし	変化なし	運動の所要時間短縮
		眼瞼下垂	変化なし	変化なし	変化なし		
		電気生理学的所見	M 波減衰率改善	未検	未検	M 波減衰率改善	未検
筋生検	施行年齢／部位		9 歳 4 カ月／右上腕二頭筋	12 歳 2 カ月／右上腕二頭筋	11 歳／左上腕二頭筋	未検	6 歳 11 カ月／左上腕二頭筋
	結果		type 2B 線維減少 type 2C 線維増加	type 1 線維増加 type 2C 線維増加	神経筋接合部の non specific enolase 染色陰性	未検	type 1 線維増加 type 2B 線維欠損

NE：未実施，RNS：反復神経刺激

動ではなかったが，自宅の階段を2階まで昇れる日と昇れない日があった．症例5は15分程度の歩行で動揺性歩行と頭部前屈を認める日，2時間の歩行で動揺性歩行を認める日，10階まで階段を昇っても疲労を呈さない日を認めた．3例とも変動の明らかな誘因や周期性は認めなかった．次に長期変動の特徴について述べる．症例1では疲労によって数日間続く歩行距離の短縮を認めた．症例3ではマラソンなどの長時間の運動負荷後に数日間続く疲労と筋力低下を認めた．また，筋力低下は伴わなかったが，数カ月の周期で易疲労感の増悪と軽減を自覚していた．症例4は感冒罹患や喘息発作から1週間後に立位保持困難となり1週間かけて徐々に回復する筋力の変動を認めた．日によって異なる筋力変動と長期変動は休息による回復を認めなかった．

2. 検査所見（表2）

1）反復神経刺激（図1a～e）

評価はそれぞれ9歳3カ月時（症例1），12歳2カ月時（症例2），19歳時（症例3），6歳10カ月時（症例4），6歳11カ月時（症例5）に行った．遠位の運動神経では正中神経を刺激した2例（症例1，症例4）のうち1例（症例1），腓骨神経を刺激した3例のうち1例（症例5）で減衰を認めなかった．症例2の尺骨神経では通常の反復刺激ではrepetitive CMAPを認めたが，減衰を認めず，30秒間手掌を強く握らせた後に刺激したところ第4反応で82%の減衰を認めた．近位の運動神経である副神経では評価した3例全例が減衰した．

2）塩酸エドロフォニウム試験

塩酸エドロフォニウム試験は投与後のCMAP減衰率の改善を2例で認め，陽性と判定した．また，投与後の運動負荷への所要時間の短縮を認めた1例を陽性，呼吸不全を呈した1例を悪化と判定した．眼瞼下垂の改善を認めた例はなかった．

3）自己抗体，筋生検，遺伝子変異

抗AChR抗体，抗MuSK抗体は検索した全例で陰性であった．筋生検は施行した4例全てで非特異的所見であったが，症例3ではCMSと診断された後に神経筋接合部のnon specific enolase染色を行ったところ，欠損を認めた．遺伝子変異は*DOK7*変異1例（症例1），*COLQ*変異3例（症例2，3，5），*CHRNE*変異1例（症例4）であった．

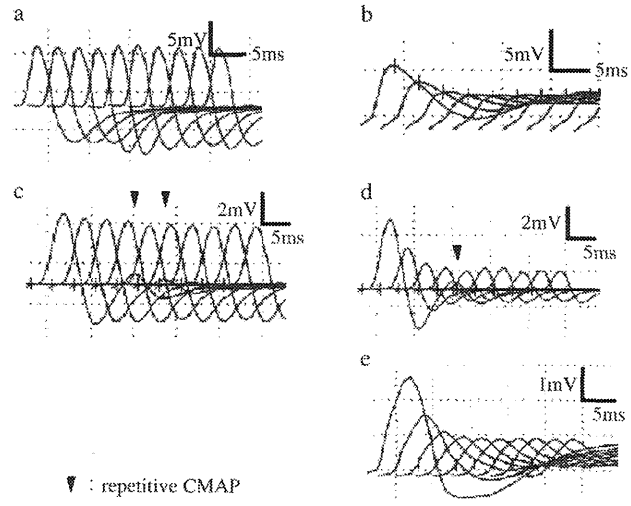

図1 反復神経刺激結果（症例1，症例2）

a：症例1の右正中神経3 Hz刺激 有意な減衰を認めなかった．
b：症例1の副神経3 Hz刺激 第4反応で83%の減衰を認めた．
c：症例2の左尺骨神経3 Hz刺激 repetitive CMAP（矢頭）を認めたが有意な減衰を認めなかった．
d：症例2の強収縮後の左尺骨神経10 Hz刺激 repetitive CMAP（矢頭）と第4反応での82%の減衰を認めた．
e：症例2の右副神経3 Hz刺激 第4反応で78%の減衰を認めた．

3. 治療

*DOK7*変異例（症例1）は，pyridostigmine bromide開始後の筋力改善は明らかでなかったが，3,4-Diaminopyridine（3,4-DAP）20 mg/日の内服開始後に階段昇降の時間が短縮し，ジャ

Presented by Medical*Online

ンプが可能となった．さらにephedrine hydrochloride 20 mg/日を追加したところ，両上肢の挙上時間が10秒から20秒へ延長し，臥位から立位への体位変換に要する時間が，10秒から3～4秒に短縮した．*COLQ*変異例（症例2，3，5）は，75～100 mg/日のephedrine hydrochlorideが全例で有効であり，易疲労性，運動不耐の改善を認めた．症例2は開始後に6分間歩行距離が130 mから280 mに延長した．また，これら症例1，2，3，5の4例では筋力の変動幅も縮小した．*CHRNE*変異例（症例4）はpyridostigmine bromide 90 mg/日，3,4DAP 30 mg/日では易疲労感の若干の改善のみであったが，ephedrine hydrochloride 25 mg/日開始後からは階段昇降の所要時間が短縮した．なお，3,4DAPは試薬として販売されているため，治療目的での使用にあたっては各医療機関で倫理審査会での承認と，保護者の承諾を得た．

Ⅲ 考　　察

CMSは先天性ミオパチー，抗体陰性重症筋無力症，中枢性低緊張，代謝性疾患，先天性筋ジストロフィー，ミトコンドリア病[2)5)13)14)]と診断されている例が多く，これらの疾患との鑑別が重要である．CMSは遺伝子変異ごとに臨床症状の特徴が若干異なり，たとえば*DOK7*変異は肢帯優位に認める筋力低下[5)14)]，*COLQ*変異は小児期早期からの筋力低下，進行性の体幹の筋力低下と側彎，拘束性呼吸不全[1)]，*CHRNE*変異は新生児期発症，眼球運動制限，球麻痺，軽度の近位筋力低下，遠位筋萎縮，呼吸器感染の反復[15)16)]が特徴的な症状と報告されている．今回の症例と比較すると*COLQ*変異例（症例2，3，5）と報告での臨床像は一致していた．また，*COLQ*変異例では遺伝子変異によって重症度に差がないと報告されているが，今回の症例でも同様の傾向を認めた．Compound heterozygote変異を有する2例（症例3，5）はhomozygoteの1例（症例2）よりも軽症であったが，過去の報告[7)17)18)]では接合による重症度の違いを認めず，意義は不明であった．*DOK7*変異例（症例1）は呼吸不全，運動発達遅滞，眼瞼下垂を伴う重症例であり，*CHRNE*変異例（症例4）は球麻痺，眼瞼運動制限を伴わず，従来の報告より軽症であった．また，*DOK7*変異例は長期にわたる筋力変動を呈することがある[14)19)]が，今回の検討では*COLQ*変異例，*CHRNE*変異例も間欠的あるいは長期での筋力変動を呈し，日内変動のみを呈した例はなかった．間欠的変動，長期変動ともに眼瞼下垂の程度には変化がなかった．この筋力変動は休息によって回復しないことから易疲労性とは異なると考えられた．このような変動を呈する理由は不明であり，従来の報告でも詳細な記載が見当たらなかったが，特定の遺伝子変異と関連しているものではなく，CMSに共通した特徴的な症状であることが今回の検討により明らかとなった．

代表的な神経筋接合部の評価方法にRNSと塩酸エドロフォニウム試験がある．RNSでは近位の運動神経である副神経において評価した全例で減衰を認めたが，遠位の運動神経である正中神経，尺骨神経，脛骨神経においてCMAPの減衰を認めない例があった．Ben Ammarらは筋力低下を呈する遠位筋の支配神経に，複数回行ったRNSのうち12例中9例が1回は減衰を呈さなかったと報告しており[14)]，Mihaylovaらは近位筋，遠位筋ともに減衰を呈さなかった*COLQ*変異例2例を報告している[20)]、我々の症例でも症例1，2は遠位筋の筋力低下を認めるにもかかわらず，これらの筋を支配する運動神経のRNSは減衰を示さなかった．RNSは遠位筋，近位筋両方の支配神経で複数回行うことが重要であった．また，減衰を認めずrepetitive CMAPのみを認める例があり注意が必要であった．

塩酸エドロフォニウム試験の評価は5例中2例で眼瞼下垂を認めなかったため，負荷前後のRNS減衰率や階段昇降の所要時間を比較することで効果を判定したが，眼瞼下垂を呈する例でも塩酸エドロフォニウム試験での眼瞼下垂の改善は認めなかった．*COLQ*変異および*CHRNE*変異の病態は，それぞれ神経筋結合部におけるアセチルコリン過剰と，シナプス後領域のアセチルコリンに対する反応の延長であるため，アセチルコリンエステラーゼ阻害薬である塩酸エドロフォニウムによる眼瞼下垂の改善を認めない可能性があるが，*DOK7*変異でも眼瞼下垂の改善が見られない理由は不明であった．眼瞼下垂のみを塩酸エドロフォニウム試験の評価対象としていると，異常なしと判断する可能性が高く注意が必要である．これらの所見はCMSに特徴的な所見でありMGとの鑑別の一助となると考えた．CMSではこれまで報告されている全身の筋力低下，易疲労性，生後1年以内の発症[1)～3)]以外に，間欠的または長期的な筋力変動，近位筋支配の運動神経でのRNS減衰，眼瞼下垂を呈する例では塩酸エドロフォニウム試験で眼瞼下垂の変化を認めないことが特徴であり，原因遺伝子にかかわらず共通する症状であった．臨床的特徴と電気生理学的検査でこれらの所見があれば臨床的にCMSが強く疑われ，遺伝子検査を考慮すべきであると考える．

遺伝子解析を施行していただいた名古屋大学大学院医学系研究科・神経遺伝情報学大野欽司教授，症例4を紹介および診断いただきました瀬川小児神経学クリニック野村芳子先生，症例1を紹介いただきました聖マリアンナ医科大学病院小児科宇田川紀子先生，抗MuSK抗体測定を施行していただいた長崎大学病院神経内科本村政勝先生に深謝申し上げます．

なお，本研究は厚生労働科学研究費補助金（難治性疾患克服研究事業）「先天性筋無力症候群の診断・病態・治療法開発研究」班（研究代表者：大野欽司）および，精神・神経疾患研究開発費「筋ジストロフィーの治験拠点整備，包括的診療ガイドラインの研究」班（主任研究者：小牧宏文）の一部であり，本論文の要旨は第53回日本小児神経学会総会（2011年5月，横浜）にて発表した．

文　　献

1) Engel AG, Ohno K, Sine SM. Sleuthing molecular targets for neurological diseases at the neuromuscular junction. *Nat Rev Neurosci* 2003;**4**:339-52.

Presented by Medical*Online